Jens Bange, Thomas Spieß, Marcus Herold, Frank Beyrich, Barbara Hennemuth

Turbulent fluxes from Helipod flights above quasi-homogeneous patches within the LITFASS area

Zuerst erschienen in:
Boundary Layer Meteorology. - Dordrecht : Springer. - Bd. 121 (2006), Nr. 1, S. 127-152
The original publication is available at www.springerlink.com.
DOI: 10.1007/s10546-006-9106-0
http://www.springerlink.com/content/05j1h1741320638u/fulltext.pdf

Boundary-Layer Meteorol
DOI 10.1007/s10546-006-9106-0

RESEARCH ARTICLE

Turbulent fluxes from Helipod flights above quasi-homogeneous patches within the LITFASS area

Jens Bange · Thomas Spieß · Marcus Herold · Frank Beyrich · Barbara Hennemuth

Received: 24 May 2005 / Accepted: 22 June 2006

Abstract Turbulent fluxes of sensible and latent heat were measured with the helicopter-borne turbulence probe Helipod over a heterogeneous landscape around the Meteorological Observatory Lindenberg during the STINHO-2 and LITFASS-2003 field experiments. Besides the determination of area-averaged heat fluxes, the analysis focused on different aspects of the response of the turbulent structure of the convective boundary layer (CBL) on the surface heterogeneity. A special flight pattern was designed to study flux profiles both over quasi-homogeneous sub-areas of the study region (representing the major land use types—forest, farmland, water) and over a typical mixture of the different surfaces. Significant differences were found between the heat fluxes over the individual surfaces along flight legs at about 80 m above ground level, in agreement with large-aperture scintillometer measurements. This flux separation was still present during some flights at levels near the middle of the CBL. Different scales for the blending height and horizontal heterogeneity were calculated, but none of them could be identified as a reliable indicator of the mixing state of the lower CBL. With the exception of the flights over water, the latent heat flux measurements generally showed a larger statistical error when compared with the sensible heat flux. Correlation coefficients and integral length scales were used to characterise the interplay between the vertical transport of sensible and latent heat,

J. Bange (✉) · T. Spieß
Institute of Aerospace Systems,
Technical University of Braunschweig,
Hermann-Blenk-Str. 23, 38108, Braunschweig, Germany
e-mail: j.bange@tu-bs.de

M. Herold
Alfred-Wegener-Institute, Bremerhaven, Germany

F. Beyrich
German Meteorological Service, Lindenberg, Germany

B. Hennemuth
Max-Planck-Institute for Meteorology, Hamburg, Germany

which was found to vary between 'fairly correlated' and 'decoupled', also depending on the soil moisture conditions.

Keywords Airborne measurements · Blending height · Heterogeneous surface · Horizontal mixing · Latent heat flux · LITFASS

1 Introduction

The atmospheric flow above heterogeneous land surfaces is an important issue for numerical weather prediction and climate models. The exchange of energy between the surface and the atmospheric boundary layer (ABL) is much more complex and less understood compared to that over homogeneous terrain. The mechanisms have to be studied experimentally before they can be implemented in numerical models. The relation between the variability of the underlying surface and the vertical turbulent fluxes, e.g., the surface temperature field and the sensible heat flux, is not linear or trivial (Brunsell and Gilles 2003). Especially the required spatial and temporal model resolutions, the cornerstones and limits of any numerical study, is an important topic. The model resolution is often set by the computing resources rather than by the physical problem (Roy and Avissar 2000). Models that do not resolve the relevant scales or do not consider the vertical reach of horizontal heterogeneity cannot be able to predict properly the vertical heat transport over land surfaces that are typical of central Europe for example. The definition of the relevant scales is also an important subject for the verification of numerical results using in situ measurements (Lemone et al. 2003). Several conclusions about the minimum scale of surface heterogeneity $L_{\mathrm{het,min}}$ that influences the lower ABL have been made; e.g., Maurer and Heinemann (2006) found that aircraft measurements at 150 m were only influenced by $L_{\mathrm{het,min}} > 5$ km, in agreement with Roy and Avissar (2000).

The impact of small-scale surface heterogeneity on the spatial variation of vertical turbulent fluxes is reduced by horizontal turbulent mixing. In the lower convective boundary layer (CBL) the size of turbulent eddies increases with height, and the influence of the underlying heterogeneous surface decreases (Mahrt et al. 2001). Another approach is the examination of single (abrupt) surface changes and their effect on the atmospheric flow. For example, Morse et al. (2002) analysed the response of the turbulence development behind a forest edge, and a widespread perception is the formation of internal boundary layers (IBL) leeward of a surface change. Many experimental studies, both in laboratories and in the field, theoretical considerations and numerical simulations exist on this topic (Garratt 1990; Irvine et al. 1997; Philip 1997; Renfrew and King 2000; Klipp and Mahrt 2003; Savelyev and Taylor 2005; to name a few). However, the practical challenge is to find reliable horizontal or vertical measures that define, for example, at what height above the ground the influence of a given horizontal heterogeneity vanishes.

The data presented here were sampled by the helicopter-borne turbulence probe Helipod during two field campaigns in the LITFASS area (Lindenberg Inhomogeneous Terrain — Fluxes between Atmosphere and Surface: a long-term Study; Beyrich et al. 2002). The experimental site was located near the Meteorological Observatory Lindenberg (MOL) of the German Meteorological Service (DWD), about 60 km south-east of Berlin. The flights during the STINHO-2 experiment (Structure of the Turbulent transport above a INHOmogeneous surface) were carried out between

24 June and 10 July 2002, the flights during the LITFASS-2003 experiment between 23 May and 17 June 2003. The campaigns were part of the EVA_GRIPS (regional EVAporation at GRId/Pixel Scale over heterogeneous land surfaces) and the VERTIKO (VERTIcal transport of energy and trace gases at anchor stations under Complex natural conditions) network. About 100 flight hours were made in the ABL, mostly under convective conditions, above a heterogeneous terrain typical of central Europe (Fig. 1). Turbulent fluxes were measured on various flight patterns. For the analysis presented here only flights above larger individual homogeneous sub-areas within the heterogeneous area are considered. The results from the remaining flight patterns will be published elsewhere (e.g., Bange and Spieß 2006). The observed influence

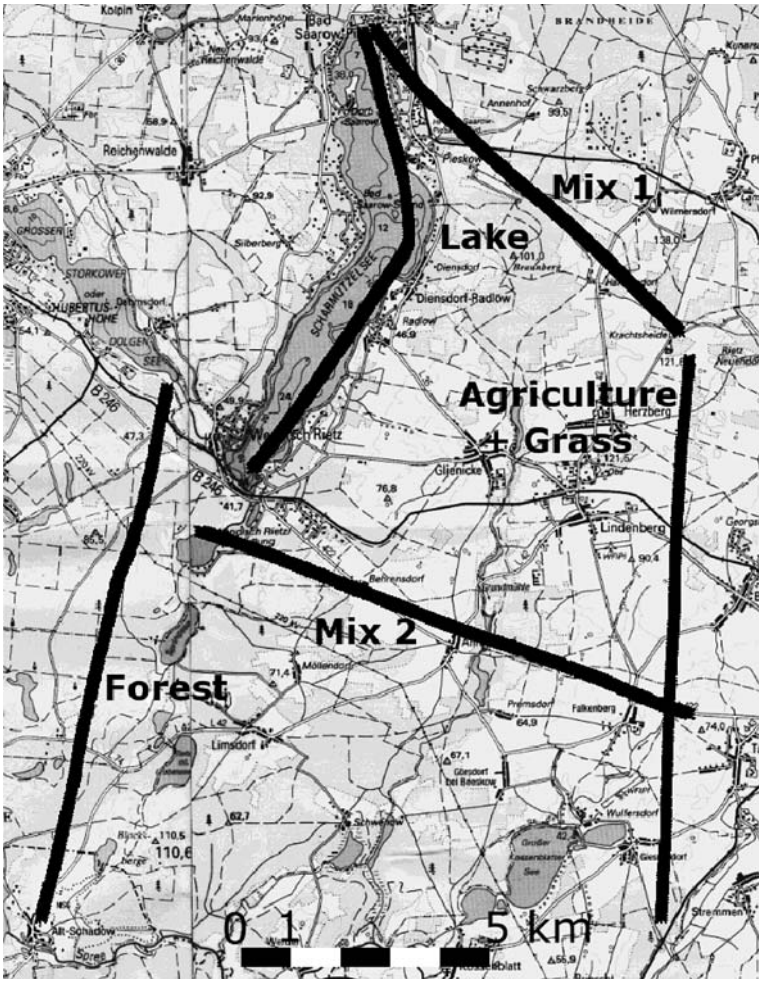

Fig. 1 Horizontal flight pattern "catalogue" flown on 6 July 2002, at about 100 m agl. The length of the legs of this type of flight pattern varied between 5 and 18 km. The legs were flown at several altitudes above homogeneous sub-areas: lake Scharmützelsee (from north to south, the leg with the kink), forest (from north to south, the leg in the west), grassland and agriculture (from north to south, the leg in the east), and a mixture of all (from west to east, two legs). Mix leg #1 was not performed on all flights. Often, the legs were flown twice (bi-directional)

of the heterogeneous land surface on the vertical profiles of turbulent heat fluxes is compared with blending height theory, CBL scaling and IBL prediction. To do so, scales discussed by Mahrt (2000) and Strunin et al. (2004) are applied. Finally, the differences between measurements of sensible heat and moisture fluxes in the CBL and theoretical considerations are clarified.

2 Experimental set-up

2.1 Instrument overview

Overviews on the STINHO-2 and LITFASS-2003 campaign can be found in Raabe et al. (2005) and Beyrich and Mengelkamp (2006). During LITFASS-2003, eddy-covariance measurements of the near-surface sensible and latent heat fluxes were made at 13 sites over different types of land use (forest, lake, grassland, various farmland). Area-averaged fluxes were determined by taking into account the data quality of the single flux values from the different sites and the relative occurrence of each surface type in the area (Beyrich et al. 2006). These so-called flux composites agreed well with the area-averaged fluxes derived from Helipod flights (Bange et al. 2006). During LITFASS-2003, long-distance large aperture scintillometers (LAS) were in operation over three different paths. A 2.85-km path represented the forested part of the study area (forest LAS), a 4.7-km path was mainly representative of farmland regions (farmland LAS), and a 10-km path (XLAS) extended over an area of mixed land use (Meijninger et al. 2005; Beyrich et al. 2006). Turbulent fluxes derived from LAS and Helipod were compared when the LAS path and the flight leg represented the same type of surface. The vertical structure of the ABL during both experiments was observed using routine radiosoundings and operational wind profiler/RASS systems at the MOL. During LITFASS-2003, information on the ABL structure was also available from two lidar systems (Linné et al. 2006) namely, a Doppler lidar (for vertical wind measurement) and a water vapour differential absorption lidar (DIAL) that measured the absolute humidity (Bösenberg and Linné 2002). Special Helipod flights were designed for comparison with the remote sensing systems.

2.2 Helipod flights

2.2.1 Measurement system

The Helipod is a helicopter-borne turbulence measurement system designed for boundary-layer field experiments over land, sea and polar regions. The sensor package is about 5 m in length, 0.5 m in diameter and 250 kg in weight. It is attached to a rope of 15-m length and can be carried by almost any helicopter. At a typical airspeed of $40\,\mathrm{m\,s^{-1}}$ the Helipod is well in front of the wake vortex of the rotor blades. Due to its small fuselage, and the absence of wings and propulsion, flow disturbance is small compared to conventional research aircraft. The Helipod carries its own navigation system, power supply, data storage and fast responding sensor equipment for in situ measurements of wind, temperature, humidity and the turbulent fluxes. During the field experiments described here the sampling rate was 100 Hz (upgraded to 500 Hz in 2005) equivalent to one measurement point every 0.4 m. More details on the Helipod can be found in Engelbart and Bange (2002), Bange et al. (2002), Muschinski et al. (2001), Roth et al. (1999), Bange and Roth (1999), Muschinski and Wode (1998).

2.2.2 Flux calculation

The vertical turbulent fluxes of sensible (H) and latent heat (λE) were determined by eddy covariance. First the turbulent fluctuations of the vertical wind w' and of the transported quantity s' (potential temperature θ or moisture mixing ratio m, respectively) were calculated by removing the mean value and the linear trend from the measured time series. Then the time series of instantaneous flux

$$f(t) = w'(t)\, s'(t) \tag{1}$$

was averaged ($\langle \ldots \rangle$) over the duration T_L for each straight and level flight leg to obtain the vertical flux

$$F = \rho\, c_s\, \langle f \rangle, \tag{2}$$

where ρ is the air density, c_s is the specific heat at constant pressure c_p or the latent heat λ of vaporisation, respectively. The statistical uncertainty (variance) of the turbulent flux according to Lenschow and Stankov (1986) is

$$\sigma_f^2 = 2\, \frac{I_f}{T_L}\, \langle f'^2 \rangle. \tag{3}$$

with the integral time scale

$$I_f = \int_0^{\tau_1} d\tau\, \frac{\left\langle f'(t+\tau)\, f'(t) \right\rangle}{\left\langle f'^2 \right\rangle}. \tag{4}$$

The integral length scale was obtained by multiplication of I_f with the true air speed $V_{\mathrm{tas}} = 40\,\mathrm{m\,s^{-1}}$ of the Helipod, assuming Taylor's hypothesis of frozen turbulence is valid. In practice I_f is calculated by integration from zero lag to the first crossing with zero τ_1 (Lenschow and Stankov 1986). Due to statistical considerations the integral scale has to exist (e.g., Lumley and Panofsky 1964, p. 37; Blackadar 1998, p. 100), but often it is reported that I_f is difficult to calculate since the autocorrelation functions behave unpredictably (e.g., Mann and Lenschow 1994; Lenschow et al. 1994) or do not cross zero at reasonable times (Lumley and Panofsky 1964). Remarkably, all Helipod flux measurements during STINHO-2 and LITFASS-2003 allowed a proper calculation of I_f without any approximation (Bange et al. 2006).

2.2.3 Flight strategy

The heterogeneous study area consisted of patches of different land use with length scales between a few tens of metres and several kilometres (Beyrich and Mengelkamp 2006). Within this mosaic there were larger quasi-homogeneous areas of rather uniform land use, called 'homogeneous sub-areas' in the following. With a special flight strategy we studied the fluxes both over these homogeneous sub-areas and over a typical mixture of the different surface types. For this, the flight legs had to be located above the homogeneous surface segments. To obtain an acceptable statistical flux error, the averaging length (the flight distance) had to be as large as possible (Lenschow and Stankov 1986). On the other hand the flight legs had to be located within the segments of interest. Therefore, only the largest sub-areas were chosen to determine the turbulent fluxes of the main surface types forest, lake and farmland. As a fourth

Table 1 List of catalogue flights during STINHO-2 and LITFASS-2003

Name	Date	Time (UTC)	Number of legs	Altitude agl (m)	Clouds (N/8)
S7	5 July 02	1123–1404	3 × 6	70, 535, 1200	6 Cu
S10	6 July 02	0724–1051	4 × 6	100, 460, 1100	2-5 Ac, 6 Ci
S12	8 July 02	0955–1216	3 × 6	90, 450, 1100	2-4 Cu
S13	8 July 02	1221–1438	3 × 6	100, 355, 920	3-4 Cu
L11	30 May 03	0808–1020	19	90, 715	No clouds
L12	30 May 03	1224–1432	17	90, 720	No clouds
L13	2 June 03	0919–1137	17	100, 550	4-5 Cu, 1 Ac, 1 Ci
L30	13 June 03	1217–1318	7	80	1 Cu
L32	14 June 03	0827–0925	11	80	1 Cu, 7 Ci

surface type the mixture of forest, farmland and lake was defined. The mixed terrain contained small patches of all types representing a surface with its own attributes, as demonstrated in Sect. 3. Flight measurements were located so that they were only influenced by one of the surface types (Fig. 1, 'catalogue' flights). The lowest flight level z_1 of a catalogue flight was placed between 80 and 150 m, the second (z_2) close to the middle of the CBL, typically between 400 and 800 m (Table 1). The consideration of the footprint — the influence of the surrounding terrain on the measurement location — was necessary, especially at the lowest flight level. At 100 m height the footprint area was expected to be less than 1 km upstream, since both field campaigns were characterised by low wind speeds. The horizontal drift of the air mass was considered by moving the flight legs leeward to the edge of the homogeneous sub-area. For instance, the leg above lake Scharmützelsee (Fig. 1) was moved to the eastern (western) shore when the mean wind was from western (eastern) directions.

Surface fluxes that were representative for the entire experimental area were derived from catalogue flights using the low-level flight and inverse model method (LLF + IM; Bange et al. 2006). The method is based on solving the enthalpy equation at a low flight level using inverse models (Wolff and Bange 2000). The obtained flux divergences were then used to extrapolate the fluxes measured at z_1 to the ground. The LLF + IM method does not work for single legs. The surface fluxes of individual sub-areas were determined by linear extrapolation of turbulent fluxes measured at z_1 and z_2.

3 Results

Nine catalogue flights were performed during the LITFASS-2003 and STINHO-2 experiments (Table 1), seven of them at more than one altitude within the CBL and suited for further analysis of the vertical CBL structure (Table 2). During these flights, the vertical CBL structure was continuously monitored by ground-based remote sensing instruments. The CBL height z_i was derived from lidar or wind profiler measurements, and only for the flight L13 on 2 June 2003 could the CBL top not be determined accurately.

For the observed CBL a linear vertical profile of the mean sensible heat flux H was assumed, so the linear interpolation of flux measurements at two or more heights provided an estimate of the flux divergence and therefore of the surface flux of sensible heat. In Fig. 2 the method was applied to two catalogue flights at two altitudes each, both performed on 30 May 2003 (flights L11 and L12 in Table 1). This day was

Table 2 Parameters of all catalogue flights at the second flight level z_2 during STINHO-2 and LITFASS-2003

Number	S7	S10	S12	S13	L11	L12	L13
Date	5 July 02	6 July 02	8 July 02	8 July 02	30 May 03	30 May 03	2 June 03
Start time UTC	1200	0945	1030	1350	0910	1330	1021
End time UTC	1237	1015	1100	1400	1020	1432	1101
z_i [m]	1300	1000	1600	1850	1200	1750	≈ 1700
$\bar{u}(z_1)$ ($\mathrm{m\,s^{-1}}$)	3.52	2.31	4.28	4.72	3.21	2.58	4.05
Wind direction (deg)	206	166	172	181	98	142	122
$\bar{\theta}$ (K)	293.3	294.1	296.3	298.3	292.5	297.3	297.3
σ_{T_0} (K)	2.52	2.15	3.64	4.29	4.03	6.02	5.24
σ_w ($\mathrm{m\,s^{-1}}$) at z_2	0.89	0.77	1.43	1.26	1.25	1.25	1.68
H_0 ($\mathrm{W\,m^{-2}}$)	106	164	251	237	237	274	264
u_* ($\mathrm{m\,s^{-1}}$)	0.43	0.31	0.48	0.6	0.47	0.35	0.43
w_* ($\mathrm{m\,s^{-1}}$)	1.54	1.63	2.19	2.25	1.96	2.33	2.28
I_H (m)	47–157	29–88	72–160	45–110	50–215	64–135	110–139
z_{blend} (m)	248	300	209	269	357	306	187
z_{th} (m)	263	618	508	432	648	917	563
L_{Rau} (km)	2.38	1.13	2.50	3.10	1.57	1.55	2.42
L_{RT} (km)	1.49	0.83	1.09	1.16	0.61	0.41	0.74
h_{IBL} (m)	378	502	502	399	585	728	623
h_T (m)	85.9	73.1	122.9	143.8	137.8	202.5	176.3
P_s	1.19	0.56	0.57	0.76	0.58	0.38	0.48
P_{sL}	0.62	0.22	0.36	0.56	0.28	0.27	0.33
z_2 (m)	535	460	450	355	715	720	540
mixed at z_2	YES	YES	NO	NO	NO	YES	NO
z_2/z_{blend}	2.2	1.5	2.2	1.3	2.0	2.4	2.9
z_2/z_{th}	2.0	0.7	0.9	0.8	1.1	0.8	1.0
z_2/h_{IBL}	1.4	0.9	0.9	0.9	1.2	1.0	0.9
z_2/h_T	6.2	6.3	3.7	2.5	5.2	3.6	3.1

The surface temperature and heat flux were extracted from the mixed legs only. All surface values were derived from the lowest flight level z_1

characterised by fair weather with 26°C maximum air temperature (at 2 m) in the afternoon, while the mean wind speed in the CBL did not exceed $5\,\mathrm{m\,s^{-1}}$. The maximum cloud cover was 2/8, but most of the day was cloudless, with a capping inversion maintained by large-scale subsidence.

The extrapolated flight measurements agreed well with the averaged LAS observations during the same 2-h period in the afternoon (flight L12, Fig. 2, upper panel). Good agreement was also found for the very-long distance scintillometer (the XLAS over the mixed surface), although these measurements were somewhat uncertain due to potential saturation effects on that day (Kohsiek et al. 2005). At the lowest flight and at the surface level a clear separation between fluxes over lake Scharmützelsee (close to zero), farmland and mixed surface ($200\,\mathrm{W\,m^{-2}}$ each) and forest ($400\,\mathrm{W\,m^{-2}}$) was identified. Similar flux separation above heterogeneous terrain was already observed during other flight experiments at $0.13 z_i$ (Bange et al. 2002) and 150 m agl (Bange et al. 2004; Maurer and Heinemann 2006). At the second flight level (about 750 m agl) this separation almost disappeared, although the flux above the lake was still clearly disjointed. Also the flux above the forest was about 50% smaller than the flux above the mixed area and the farmland. At this time the CBL height $z_i \approx 1700$ m (lidar

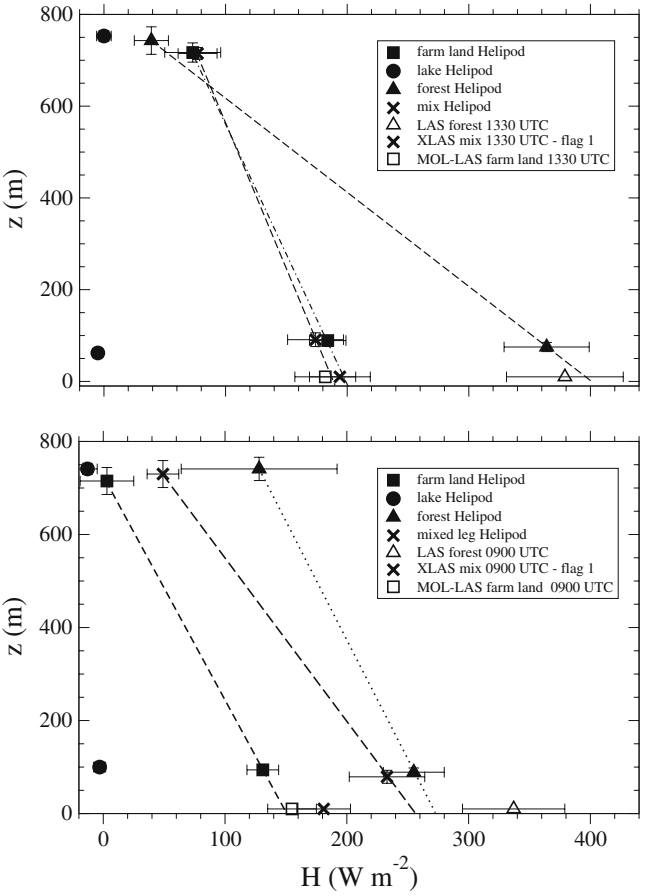

Fig. 2 Sensible heat fluxes from catalogue flight and LAS including the statistical errors, sampled on two exemplary days during LITFASS-2003. Upper panel: afternoon of 30 May 2003 (flight L12). Lower panel: same day in the morning (flight L11). Remark: The error bars of the flights above the lake are smaller than the symbol. The quality flag 1 (XLAS) indicates that the measurement was afflicted with large uncertainty in terms of data quality assurance

observation, method according to Lammert and Bösenberg 2006), so the flights were performed at about $0.44z_i$.

A quite different situation was found during the late morning flight (L11, Fig. 2, lower panel). Again, at 100 m agl the fluxes above the lake (close to zero), farmland (130 W m^{-2}), mixed land (235 W m^{-2}) and forest (260 W m^{-2}) were clearly defined by the different surface types. During the flight at the second level (at about 750-m agl, $0.6z_i$) the top of the CBL was between 1200 m and 1300 m. Also at the second level a clear separation of the turbulent fluxes was observed: -10 W m^{-2} over lake Scharmützelsee, close to zero over farmland, 50 W m^{-2} over mixed land, and 130 W m^{-2} over forest. With the exception of the latter, the statistical error bars σ_H (3) were remarkably small. Hence, the CBL was not well mixed at $0.6z_i$, just before solar noon. Each homogeneous sub-area developed its own heat flux profile with individual slope (flux divergence) up to the middle of the CBL, and the linear extrapolation to the ground led to good agreement with the LAS observations over farmland. The agreement for

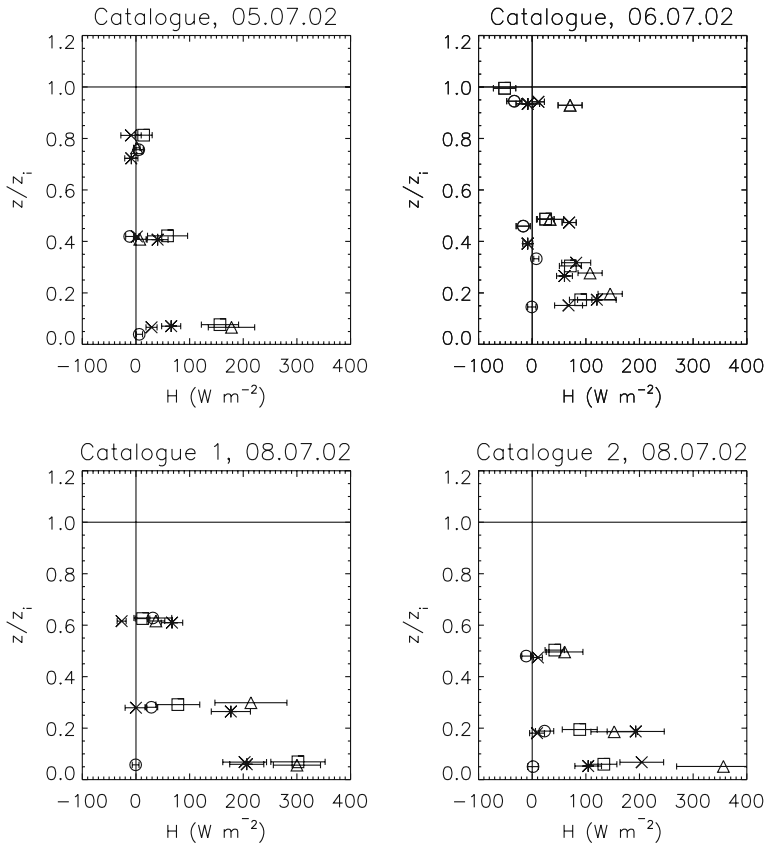

Fig. 3 Vertical profiles of sensible heat flux measurements on catalogue flights during STINHO-2. From top left to bottom right: flight S7, S10, S12, S13. The symbols indicate the underlying surface type: squares for farmland; circles for lake Scharmützelsee, triangles for forest; crosses for the mixed terrain #2, stars for the mixed terrain #1 (see Fig. 1)

the forest was not that good, but still within the statistical uncertainty. Larger differences were found with the XLAS over mixed land, though the XLAS measurements were afflicted with a larger uncertainty.

The sensible and latent heat flux measurements from all seven catalogue flights are displayed in Figs. 3–6. Here, the altitude was scaled with the inversion height z_i as identified in the remote sensing data during the flights (see also Hennemuth and Lammert 2005; Lammert and Bösenberg 2006). No major orographic features existed in the LITFASS area, and heterogeneity was mainly caused by differences in land use, which was assumed to have a small effect only on the boundary-layer top. Larger variations of z_i in the lidar time series were caused by large convective elements that were disconnected from specific locations (Uhlenbrock et al. 2004). Comparison of the CBL height estimates derived from the lidar and wind-profiler systems at Falkenberg and MOL sites (5 km apart from each other) show that these were broadly consistent (Beyrich and Mengelkamp 2006), so we assumed the lidar estimates of z_i to be representative for the study region.

The airborne latent heat flux measurements were afflicted with larger statistical uncertainty than H, and the corresponding error bars ranged from very small on most

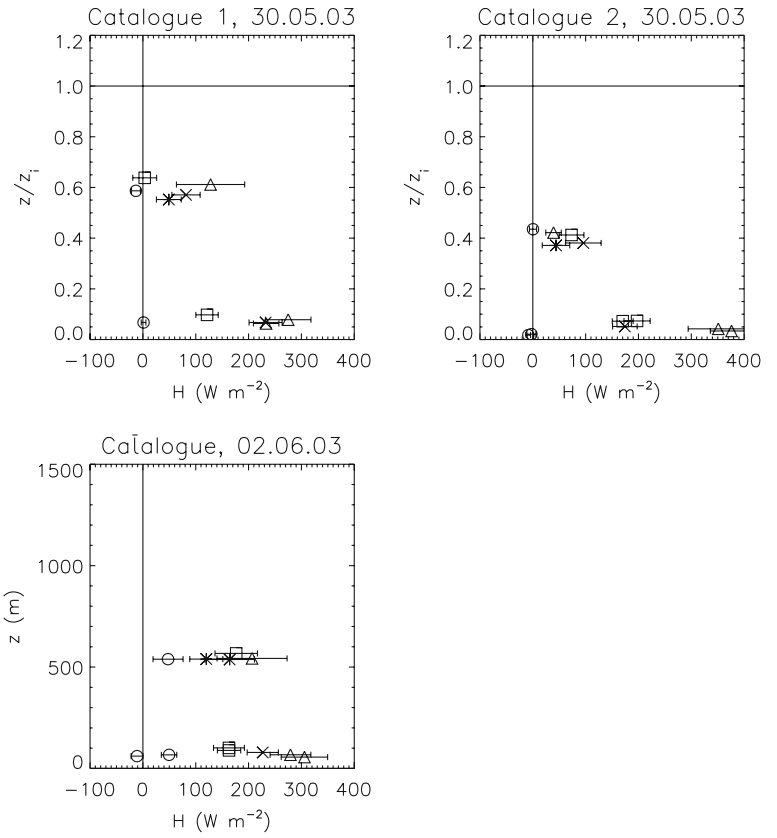

Fig. 4 Vertical profiles of sensible heat flux measured during LITFASS-2003. From top left to bottom: flight L11, L12, L13. For the explanation of the symbols see Fig. 3

of the lowest-level flights, to large in the middle of the CBL, and to unacceptable near the CBL top. On some days (for example, 5 July 2002) the statistical errors were consistently small, on other days (for example, 2 June 2003) very large at all altitudes. A systematic dependence of the moisture flux on the underlying surface type could not be identified—albeit during some flights (best example: S13) the fluxes above individual surfaces were clearly dissimilar, as well as in the middle of the CBL. Extrapolations to the surface were not made since linear or other simple height dependences could not be assumed. The different behaviour of sensible and latent heat fluxes during both experiments is discussed in Sect. 5.

4 Discussion: horizontal mixing of the CBL

4.1 How mixed was the CBL?

At the lowest flight level z_1 (70–100 m agl) the sensible heat fluxes H above the individual surface types were always clearly dissimilar, and analysis of the catalogue flights at the second level z_2 (about $0.3z_i$ to $0.6z_i$) disclosed two types of vertical flux profiles. One was the well mixed boundary layer, where airborne measurement at z_2

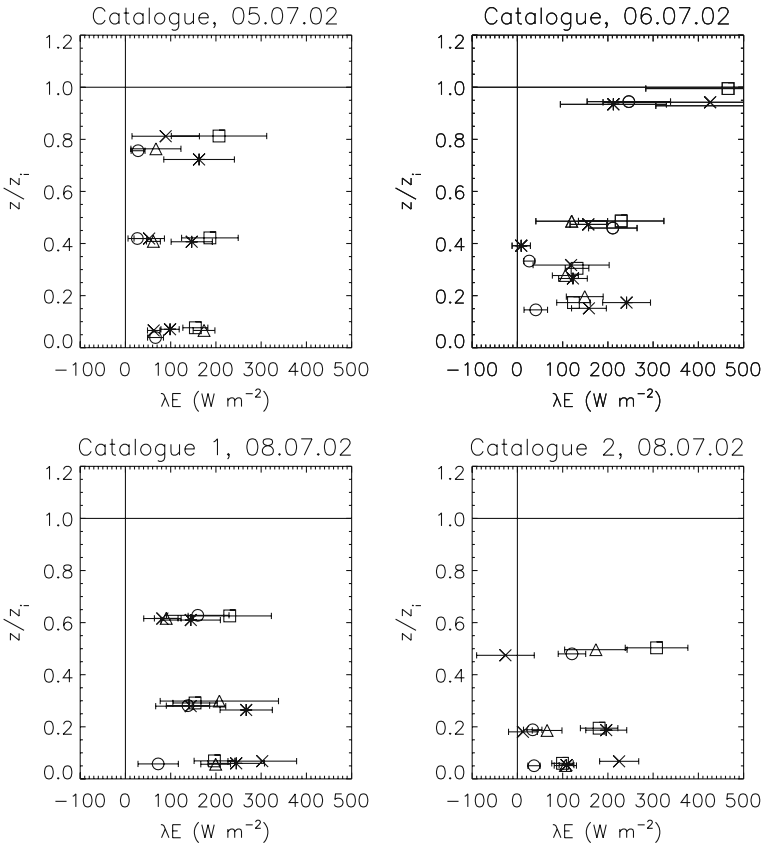

Fig. 5 Vertical profiles of latent heat flux measurements on catalogue flights during STINHO-2. From top left to bottom right: flight S7, S10, S12, S13. For the explanation of the symbols, see Fig. 3

and above led to identical sensible heat fluxes H (within the statistical uncertainty) for all surface types. The influence of the different surfaces on the heat flux vanished at these heights or was not significant anymore. In fact, the flux H above the lake was always close to zero or even negative at all flown altitudes, no matter what amount of heat flux was produced by the surrounding land surfaces.

The second type of CBL was characterised by a vertical sensible heat flux profile that still exhibited a dependence on the underlying surface at z_2 (flights S12, S13, L11, L13 in Figs. 3 and 4). The error bars of neighbouring data points often overlap, though most fluxes were clearly separated. Table 2 gives more details on the catalogue flights and indicates whether the sensible heat flux at the second flight level z_2 exhibited significant horizontal variability or not.

The horizontal variability of the latent heat flux λE did not show any systematic dependence on height. This agrees with the perception that the latent heat flux was not as connected to local surface structures as the sensible heat flux. From other experiments it has been reported that the surface moisture flux varied 'in a less organised fashion' compared to the sensible heat flux at ground level (Mahrt 2000). Flamant et al. (1997) found that λE was less connected to convective structures (which can be

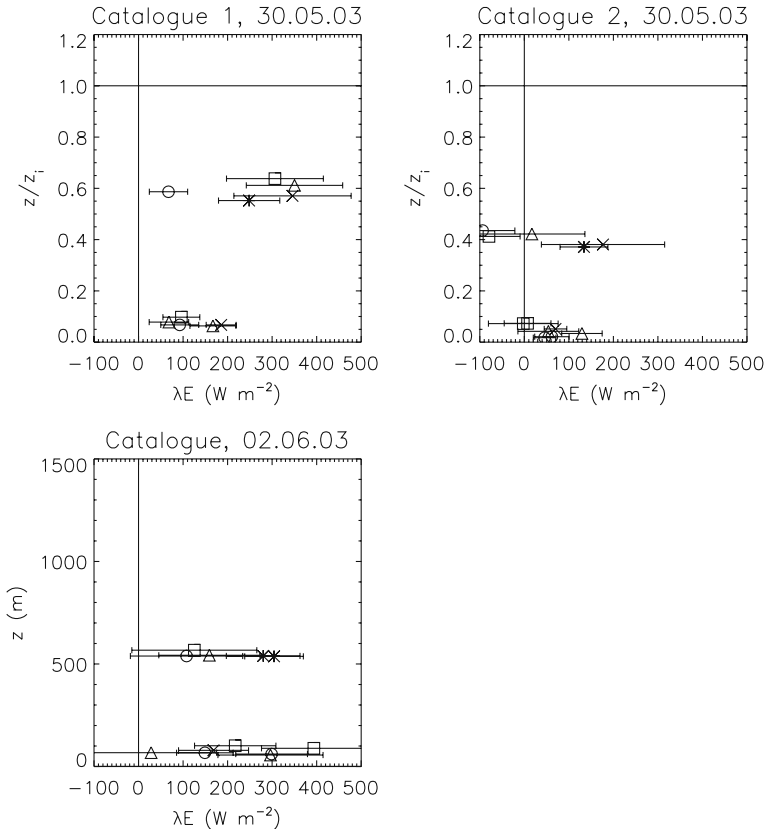

Fig. 6 Vertical profiles of latent heat flux measured during LITFASS-2003. From top left to bottom: flight L11, L12, L13. For the explanation of the symbols see Fig. 3

linked to the surface heat structure) but rather to larger scales, and that the latent heat flux profiles behaved more erratically. As long as there is no condensation humidity is often regarded as a passive tracer and subject to horizontal transport. It can therefore be assumed that the turbulent latent heat flux was to an important extent caused by horizontal humidity advection in addition to local production. The difference between latent and sensible heat fluxes is further discussed in Sect. 5.

4.2 Vertical and horizontal scales

It is apparent that several boundary parameters should indicate whether the sensible heat flux near the centre of the CBL shows horizontal variability due to the heterogeneous surface or not. For instance, the mixing state of the CBL may depend on the mean wind speed, wind direction, time of day, cloudiness, the height of the CBL and the surface sensible heat flux. In fact, we did not find any parameter that consequently distinguished horizontally mixed from non-mixed flows. Therefore a scaling length or height was sought that would do so. In the following, blending heights and horizontal scales, mainly as discussed by Mahrt (2000) and Strunin et al. (2004), are evaluated from the STINHO-2 and LITFASS-2003 flight data, and the results are

listed in Table 2. An important quantity in this analysis is the scale of heterogeneity L_{het}, identified as a characteristic scale of land patches of different roughness, surface temperature, water content, etc. To calculate the upper estimate, i.e., to give an estimate of the maximum altitude at which the surface influence was still probable, L_{het} was set to 10 km. This was the maximum diameter of the largest homogeneous patch in the experimental area, i.e., the forest in the west (Fig. 1).

4.2.1 Integral length scale

For each catalogue flight the integral scale I_H (4) of the sensible heat flux at flight level z_2 was determined. Since I_H varied considerably, the corresponding range is given in Table 2, though neither this range nor the mean integral scale depended on the underlying surface.

4.2.2 Blending height

The blending height concept (Wieringa 1986; Claussen 1991) defines a height z_{blend} within the CBL, above which the influence of the surface structure vanishes or falls below a certain threshold. Mahrt (2000) emphasises that the blending height should not be interpreted as a sharp boundary but acts as a scale that describes the vertical influence of the surface under given conditions (surface temperature, heating, roughness length, boundary-layer height, etc.). This is how most of the following scales should be interpreted.

The blending height z_{blend} increases linearly with the horizontal scale L_{het} of the surface heterogeneity, viz:

$$z_{\mathrm{blend}} = \left(\frac{u_*}{\bar{u}_0}\right)^2 \frac{L_{\mathrm{het}}}{C_{\mathrm{blend}}} \tag{5}$$

with $C_{\mathrm{blend}} \approx 0.6$ (Mahrt 2000). Here, u_* is the friction velocity and $\bar{u}_0$ the mean horizontal wind at z_{blend}. Below z_{blend} the turbulent boundary layer is not in equilibrium and therefore not horizontally mixed. Since u_* is defined in the surface layer, and $\bar{u}_0$ at z_{blend}, both cannot exactly be derived from our airborne measurements. Instead, we use two approaches to estimate the blending height.

For the given situation in STINHO-2 and LITFASS-2003 we assume $\bar{u}_0 \approx 3\,\mathrm{m\,s^{-1}}$ and $u_* \approx 0.3\,\mathrm{m\,s^{-1}}$ to estimate a typical value of z_{blend}. We obtain $z_{\mathrm{blend}} \approx 167$ m in agreement with other field experiments (e.g., Kalthoff et al. 1993; Strunin et al. 2004). In our data the sensible heat fluxes showed a clear dependence on the underlying surface at $z_1 \approx 100$ m, in agreement with the above considerations. But in four cases this dependence was still visible clearly above the estimated z_{blend} (at z_2, see Table 2).

The second approach uses the result of the preceding estimation. Since z_1 was located near the estimated z_{blend}, the measurements at z_1 were used to calculate $\bar{u}_0$ and the friction velocity

$$u_*^4 \approx \overline{w'u'}^2 + \overline{w'v'}^2 \Big|_{z_1}. \tag{6}$$

In doing so, the calculated z_{blend} exceeded the estimated blending height by a factor of between 1.1 and 2.1 (Table 2). It has to be remarked that the applied method provided only rough estimates, since the blending height concept was not applied in its original

form. Furthermore, u_* varied by about 30% during a flight, depending on the underlying surface (mean value of u_* above farmland: $0.40\,\mathrm{m\,s^{-1}}$; lake Scharmützelsee: $0.32\,\mathrm{m\,s^{-1}}$; mixed surface: $0.47\,\mathrm{m\,s^{-1}}$; forest: $0.57\,\mathrm{m\,s^{-1}}$). However, the comparison of the normalised flight level z_2/z_{blend} with the variability of H yields no correlation (Table 2). During half of the flights a mixed CBL was not found significantly above z_{blend}. The blending height concept that considers only mechanical mixing was not valid for the data discussed here, in agreement with the observations of Strunin et al. (2004).

4.2.3 Thermal blending height

Similarly to the mechanical blending height, the thermal blending height considers the thermal heating instead of the mechanical friction at the surface. Below

$$z_{\mathrm{th}} = \left(\frac{H_0}{\rho\, c_p\, \bar{u}_0\, \bar{\theta}} \right) \frac{L_{\mathrm{het}}}{C_{\mathrm{th}}}, \tag{7}$$

(with $C_{\mathrm{th}} \approx 3.1 \times 10^{-3}$; Mahrt 2000) the influence of the heterogeneous surface is still visible. Here H_0 is the area-averaged surface heat flux that was derived from Helipod measurements by application of the LLF + IM method to all legs of the corresponding catalogue flight. Wind speed $\bar{u}_0$ was again estimated from measurements at the lowest flight level. The results for z_{th} are listed in Table 2, and in four cases the observations agreed with the above considerations:

$$z_{\mathrm{th}} < z_2 \longrightarrow \text{ mixed at } z_2 \text{ (true in S7)}$$
$$z_{\mathrm{th}} > z_2 \longrightarrow \text{ non-mixed at } z_2 \text{ (true in S12, S13, L13),}$$

but disagreed in three cases (S10, L11, L12). So the thermal blending height was not a reliable indicator of horizontal mixing.

4.2.4 Raupach length

Raupach and Finnigan (1995) derived a length scale L_{Rau} based on the convective mixing time scale z_i/w_*, using the Deardorff velocity scale w_*:

$$w_*^3 = \left(\frac{g\, z_i}{\bar{\theta}} \right) \frac{H_0}{\rho\, c_p}. \tag{8}$$

During this time scale the convective flow travels the horizontal distance

$$L_{\mathrm{Rau}} = C_{\mathrm{Rau}}\, \frac{\bar{u}}{w_*} z_i \tag{9}$$

due to the mean horizontal wind speed $\bar{u}$ (where we take $C_{\mathrm{Rau}} = 0.8$). For horizontal scales $L_{\mathrm{het}} < L_{\mathrm{Rau}}$ the influence of the horizontal heterogeneity is confined to shallow depths small compared to z_i, due to horizontal convective mixing, i.e., for a large length L_{Rau} no influence of the heterogeneous surface at z_2 is expected, while for $L_{\mathrm{Rau}} \ll L_{\mathrm{het}}$ a clear separation between fluxes from different surfaces should be observed. Additionally, mesoscale thermal internal boundary layers (MTIBL, Strunin et al. 2004) may only occur when the ratio $L_{\mathrm{Rau}}/L_{\mathrm{het}}$ drops below 0.3. The results for w_* and L_{Rau} are listed in Table 2. The mean horizontal wind was approximated by the

wind speed at $z_1 \approx 100$ m. First off, for all runs L_{Rau} was on the order of those found by Strunin et al. (2004) but clearly smaller than the estimated horizontal heterogeneity scale $L_{\mathrm{het}} \approx 10$ km. Since L_{het} was an estimated scale and possibly chosen as too large, a relative comparison of the determined L_{Rau} with the state of mixing appeared to be useful. However, the flight that revealed the largest L_{Rau} (3.1 km on flight S13) exhibited clearly no horizontally mixed heat fluxes at $z_2 \approx 0.2 z_i$, in conflict with the assumption. The smallest L_{Rau} (1.13 km) was found for flight S10, which exhibited a quite well-mixed flow at $0.3 z_i$. Thus L_{Rau} was not a suitable indicator of horizontal mixing.

4.2.5 Internal boundary layers

Another approach to treating the horizontal mixing in the ABL considers the formulation of internal boundary layers (IBL). With maximum patch sizes of a few kilometres the small-scale local IBL is typical (Mahrt 2000), which is characterised by a depth h_{IBL} that is small compared to the height z_i of the CBL. The maximum height of such an IBL is (Mahrt 1996)

$$h_{\mathrm{IBL}} = C_{\mathrm{IBL}} \frac{\sigma_w}{\bar{u}} L_{\mathrm{het}} \tag{10}$$

with $C_{\mathrm{IBL}} \approx 0.15$ (Mahrt 2000). The standard deviation σ_w of the vertical wind is a measure of turbulent vertical mixing, and it varies with height but has a broad maximum between $0.2 z_i$ and $0.6 z_i$ where the variations are small (Kaimal and Finnigan 1994). Thus σ_w was calculated for each individual flight leg at z_2 and then averaged over all legs at this altitude (Table 2). With only two exceptions (S7 and L11) the second flight level z_2 was within a 10% vicinity of h_{IBL}. This was a disadvantageous condition to determine a dependence of the mixing state of the CBL on z_2/h_{IBL}. However, on flight S7 the CBL was mixed as expected ($z_2/h_{\mathrm{IBL}} = 1.4$), while it was not mixed on flight L11 ($z_2/h_{\mathrm{IBL}} = 1.2$). For the presented data, the maximum internal boundary-layer height h_{IBL} was not a good indicator of the mixing state of the CBL.

A thermal counterpart to (10) can be defined as the scale

$$h_T = \frac{\sigma_{T_0}}{\bar{\theta}} L_{\mathrm{het}} \tag{11}$$

where σ_{T_0} is the standard deviation of the averaged surface temperatures T_0 of the individual homogeneous sub-areas. So σ_{T_0} is a measure of the thermal heterogeneity of the surface (see also the scaling approaches in (Mahrt 2000). In most cases with a large ratio $z_2/h_T \approx 6$ the flow was found mixed, while the flow was found non-mixed when $z_2/h_T \leq 4$. This is as expected, but was unfortunately not fulfilled for the flights on 30 May 2003 (L11 and L12). In any case, (11) led to the most promising results so far.

The combination of (11) with (9) leads to another horizontal scale

$$L_{\mathrm{RT}} = C_{\mathrm{RT}} \left(\frac{\bar{\theta}}{\sigma_{T_0}} \right) \left(\frac{\bar{u}}{w_*} \right) z_i \tag{12}$$

with $C_{\mathrm{RT}} \approx 4.3 \times 10^{-3}$ (Mahrt 2000; Mahrt et al. 2001). Again for large values of L_{RT} a mixed flow should occur, but as could be expected from the analysis of L_{Rau}, no correlation with the mixing state was found.

Finally, the observed states of horizontal mixing were compared with the MTIBL indicators defined by Strunin et al. (2004). The parameter

$$P_s = \frac{u_* \bar{\theta}}{H_0} \tag{13}$$

relates shear stress and convection. This parameter can be modified by the ratio of the horizontal heterogeneity L_{het} to the CBL depth z_i resulting in

$$P_{sL} = 4P_s \frac{z_i}{L_{\text{het}}}. \tag{14}$$

Both P_s and P_{sL} indicate the possibility of MTIBL development for values smaller than unity during flights across the river Lena (Strunin et al. 2004). The results for P_s and P_{sL} applied to our flights above the heterogeneous LITFASS area are listed in Table 2. No correlation with the mixing state of the CBL at z_2 was found.

5 Discussion: sensible vs. latent heat flux

During STINHO-2 and LITFASS-2003 the individual turbulent latent heat fluxes λE had large statistical uncertainty (error bars) compared to the sensible heat flux. Similar findings were reported from the comparable REEEFA flight experiment (Maurer and Heinemann 2006). Also the variation of the latent heat flux during the catalogue flights was large, but did not depend on the underlying surface. Other studies (Flamant et al. 1997; Katul and Hsieh 1999) also found larger scales or variances for the latent heat flux than for the sensible heat flux. In the following, statistical quantities are analysed that describe these phenomena and quantify the differences in the statistical nature of latent and sensible heat fluxes.

The STINHO-2 field campaign was carried out during a period of variable weather, with a mix of sunny and rainy days, resulting in sufficient soil water (≈9% by volume). The first half of the LITFASS-2003 experiment was exceptionally dry, though on 5 and 8 June 2003 heavy rain fell during thunderstorms, providing sufficient soil water for the rest of the campaign. To analyse the correlation between vertical wind, temperature and moisture the data sampled during the catalogue flights were split into two classes: days with wet soil (all STINHO-2 catalogue flights, and L30 and L32), and days with dry soil (L11–L13).

5.1 Correlation coefficients

The cross-correlation coefficients of vertical wind and potential temperature

$$r_{w\theta} = \frac{\overline{w'\theta'}}{\sigma_w \, \sigma_\theta}, \tag{15}$$

and of vertical wind and mixing ratio

$$r_{wm} = \frac{\overline{w'm'}}{\sigma_w \, \sigma_m}, \tag{16}$$

are compared in the scatter plots of Fig. 7. On flights above wet soil (left panel) for some cases the correlations were similar (close to the diagonal), but in most cases

asymmetry was observed. When vertical wind and temperature were weakly correlated (about 0.2), r_{wm} was comparatively large (around 0.4). For larger $r_{w\theta}$ (0.5–0.7), the corresponding r_{wm} was somewhat smaller (0.35–0.6). This is in contrast to observations in the surface layer. Katul and Hsieh (1999) found for the homogeneous, unstable surface layer, and Roth and Oke (1995) for the urban surface layer in all stabilities, that $r_{w\theta} > r_{wm}$ was always valid. In our data the latter was actually found for the flights above dry soil (Fig. 7, right-hand side). As above urban and other sealed surfaces, no water was available for vertical water vapour transport. The individual correlation coefficients of our flight data did generally not depend on the underlying surface. In most cases only for the forest a high correlation of $r_{w\theta} \approx 0.6$ was identified for both dry and wet soil.

The relative transport efficiency of sensible and latent heat

$$r = \frac{r_{w\theta}}{r_{wm}} \tag{17}$$

is plotted against the normalised altitude in Fig. 8; it seems that above wet surfaces, r decreases from 1.5 at surface level to zero at $0.8z_i$, which was probably the base of the entrainment zone. No dependence on the surface type was found, except for the flights above lake Scharmützelsee, which exhibited the smallest transport efficiency. The smaller data base for flights during the days with dry soil did not show a significant dependence on height.

Since thermal structures in the CBL also transport water vapour, moisture m and temperature θ should directly be correlated. Above warm patches a larger vertical moisture flux λE can be expected, with smaller values above cooler patches. It can be assumed that the correlation

$$r_{\theta m} = \frac{\overline{\theta' m'}}{\sigma_\theta \sigma_m}. \tag{18}$$

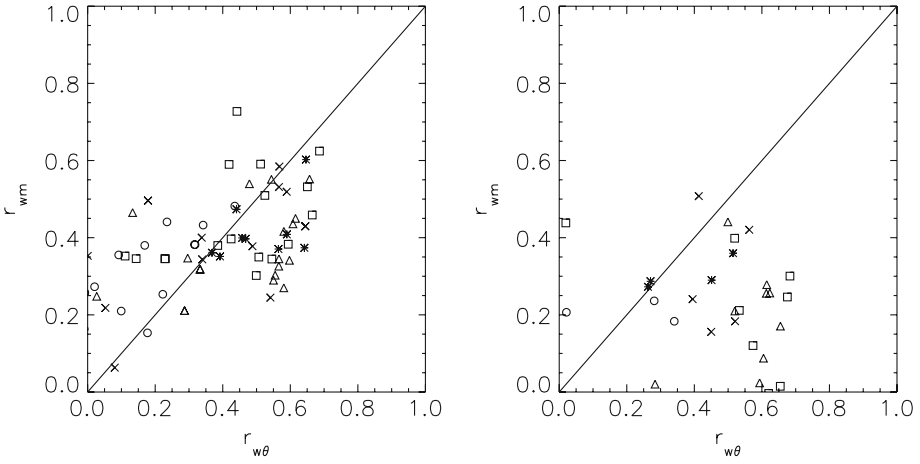

Fig. 7 The correlation coefficient of vertical wind and potential temperature versus the correlation coefficient of vertical wind and mixing ratio. Left hand side: wet soil; right hand side: dry soil. For the explanation of the symbols, see Fig. 3

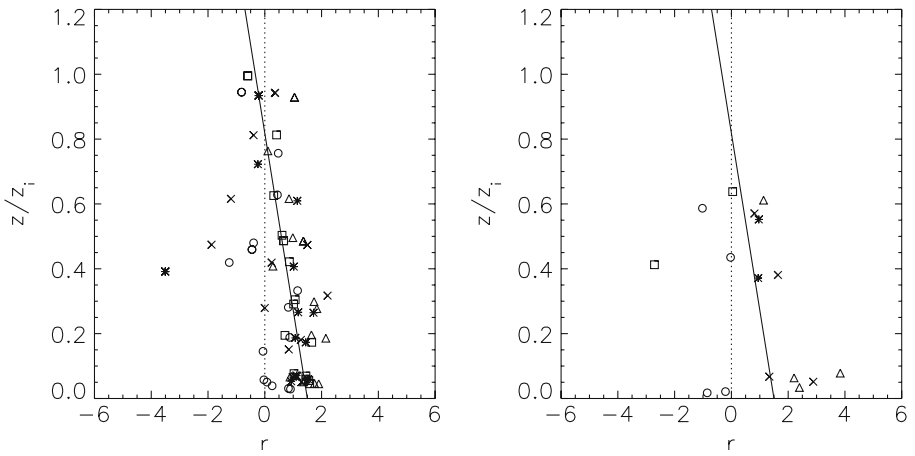

Fig. 8 The transport efficiency r vs. the normalised height. Left hand side: wet soil; right hand side: dry soil. Not for all flights the boundary layer z_i was known. Thus this diagram contains less data than Fig. 7. The solid line was fitted by eye to the data. For the explanation of the symbols, see Fig. 3

of temperature and humidity is close to unity near the surface, and since large eddies cause horizontal mixing in the centre of the CBL, $r_{\theta m}$ should decrease with height. Due to the entrainment of warm and dry air from the free atmosphere, temperature and moisture are anti-correlated near the CBL top. A more or less linear decrease of $r_{\theta m}$ with normalised height z/z_i and zero-crossing $r_{\theta m} \approx 0$ at $0.5z_i$ can therefore be assumed (Wyngaard et al. 1978).

Figure 9 reveals that the expected behaviour (dotted line) was only found in the upper part of the CBL, for $z \geq 0.6z_i$. Between $0.6z_i$ and $0.4z_i$ the correlation varied between -0.9 and 0.5, for both days with wet and dry soil. Near the wet surface the correlation between moisture and temperature was mostly found between 0.4 and 0.7, and, as expected, about zero for dry soil, but with large scatter. The absence of soil water led to low or negative $r_{\theta m}$ even at low altitudes, as also observed above urban areas (Roth and Oke 1995) where dry (wet) patches are often associated with high (low) temperatures. Lake Scharmützelsee with its low surface temperature contributed a disproportionately large latent heat flux, while the warm land patches produced only a small moisture flux since the soil contained little water.

In surface-layer experiments the dependence of r on $r_{\theta m}$, for r and $r_{\theta m}$ both positive, has been examined. Although Katul and Hsieh (1999) concluded that $r \approx r_{\theta m}$, their Fig. 2 shows that $r \geq r_{\theta m}$. Our CBL flight data expand the ranges of r and $r_{\theta m}$ to anti-correlation and clearly show that $r > r_{\theta m}$ with a few exceptions (Fig. 10). While above the wet surface r and $r_{\theta m}$ seems to be related by a linear law, no dependence was found for the dry surface. The decrease of r with increasing positive $r_{\theta m}$, as described by Roth and Oke (1995) in the urban surface layer, was not found in our data.

5.2 Integral length scales

The integral scale (4) is the 'outer' scale or macroscale of turbulent flow (Rotta 1972), and it can be interpreted as the correlation time, the persistence or memory of the turbulent flow (e.g., Kaimal and Finnigan 1994). The associated length scale can therefore

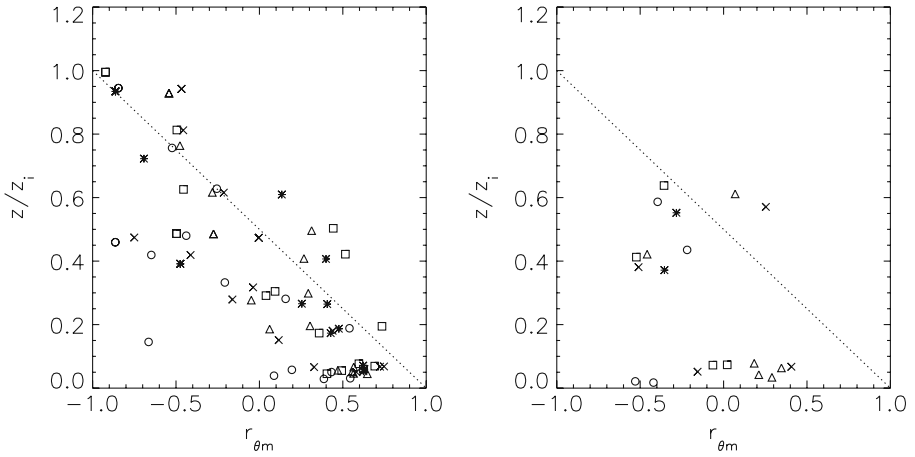

Fig. 9 The correlation coefficient of potential temperature and mixing ratio as a function of the normalised height. Left hand side: wet soil; right hand side: dry soil

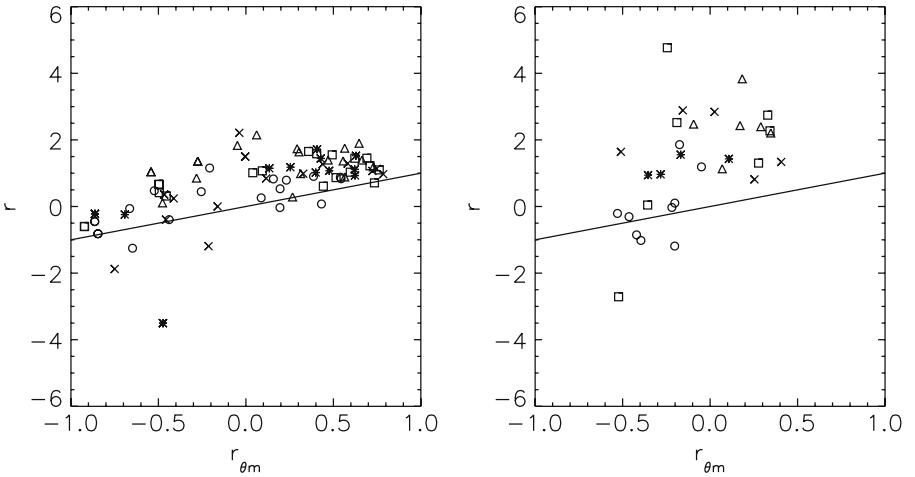

Fig. 10 The transport efficiency r versus the correlation coefficient of potential temperature and mixing ratio. Left hand side: wet soil; right hand side: dry soil. The solid lines represent $r = r_{\theta m}$

be interpreted as the typical size of the largest or most energy transporting eddies. For instance, the statistical turbulent flux error (3) is a linear function of $\sqrt{I_f}$.

As Fig. 11 reveals, in the majority of flights above soil (farmland and forest) and mixed surface the integral length scale $I_{\lambda E}$ of the latent heat flux was larger than the integral length scale I_H of the sensible heat flux. The opposite was found for flights above lake Scharmützelsee, and explains why the statistical error of the moisture flux was generally larger than the error of H, above all surfaces excluding the lake.

The ratio $I_H/I_{\lambda E}$ is plotted in Fig. 12 and 13. If different ratios during one catalogue flight at one altitude were found, then the measured fluxes did not necessarily show large horizontal variations (e.g., flights S10 and S12 at level z_2). Vice versa, if the ratios were all similar, the horizontal flux variability could nevertheless be large (e.g., S13 at level z_2). On flights above moist ground (Fig. 12) no dependence of $I_H/I_{\lambda E}$ on the underlying surface type or on the height within the CBL was found. Above

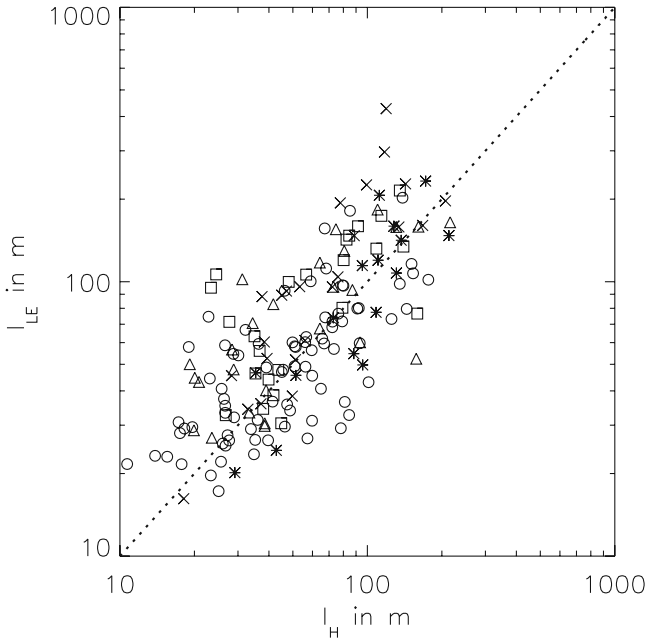

Fig. 11 Double-logarithmic scatter plot of the integral length scales of sensible and latent heat flux. The dotted line indicates $I_{\lambda E} = I_H$. The symbols are explained in Fig. 3

dry ground $I_{\lambda E}$ was clearly larger than I_H, while this difference decreased with height (Fig. 13). As a consequence the statistical error of the airborne measured moisture flux was even larger during dry periods (see Figs. 4–6).

6 Summary and conclusions

The response of the turbulent flux profiles to a patchy landscape comprising different types of underlying surface (farmland, forest, water) was analysed in the context of the field campaigns LITFASS-2003 and STINHO-2. Vertical turbulent heat fluxes were determined on flights above homogeneous sub-areas within the heterogeneous LITFASS area at several heights within the CBL. The observed distribution of different land-use types was typical of central Europe and was in no way exceptional. The extrapolation of the sensible heat flux H to the surface agreed well with LAS measurements, and clear separations in H above the individual surface types were found with the LAS and the lowest Helipod flights at 80 m. On three flights a more or less horizontally well-mixed flow was observed at the second flight level (between 350 and 720 m, or $0.2z_i$ and $0.6z_i$). On four other flights in the same altitude range, the sensible heat fluxes above the individual surfaces were still separated.

In comparison to Doran et al. (1995) the horizontal length scale of the surface heterogeneity was smaller, about 10 km, and also the geometrical distribution of the homogeneous sub-areas was more complex in our study. In agreement with Roy and Avissar (2000) and Maurer and Heienemann (2006) the 10-km heterogeneity scale had a large effect on the development of horizontal mixing in the CBL. But narrow lake Scharmützelsee (10 km × 1 km) also produced its own vertical profile of sensible

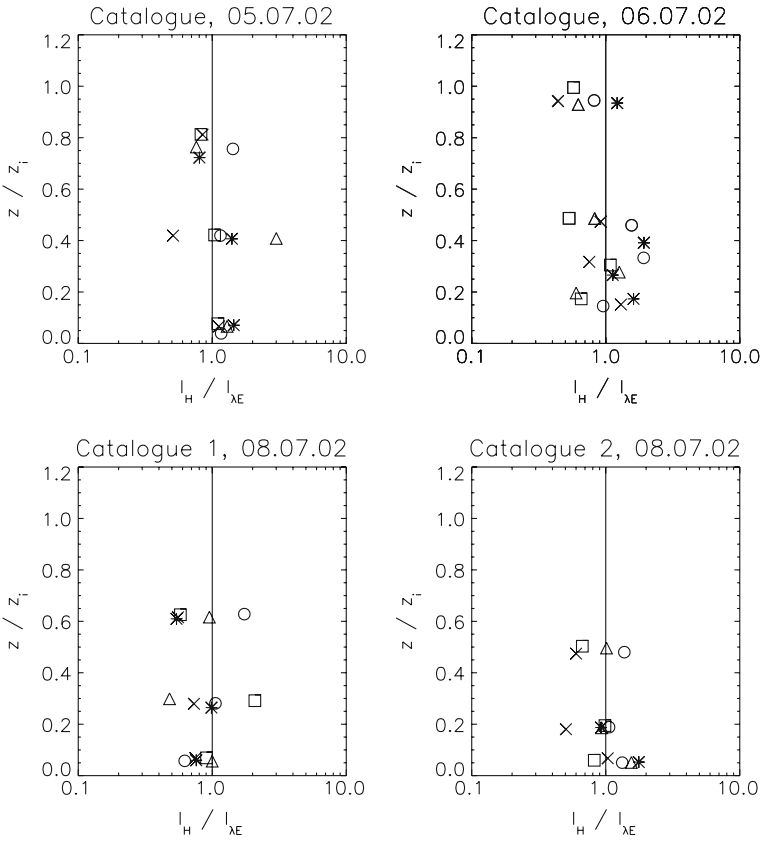

Fig. 12 Vertical profiles of the integral scale ratio observed on catalogue flights during STINHO-2. From top left to bottom right: flight S7, S10, S12, S13. For the explanation of the symbols see Fig 3

heat flux (at least in weak-wind situations) apparently unaffected by the surrounding forest and farm land.

Simple atmospheric parameters such as wind speed and direction, time of day, etc., were no indicator of the horizontal mixing state of the CBL. Therefore several vertical and horizontal scales of surface heterogeneity and their influence on the boundary-layer flow were calculated, most already discussed by Mahrt (2000) and Strunin et al. (2004) and also applied to aircraft measurements. These scales consider the mechanical or thermal heterogeneity of the terrain, and take account of the convective velocity. Although a study of seven cases is rather limited, not one of these scales was helpful in describing the mixing state of the CBL. Best results were achieved with a scale that considered the variance of the surface temperature, to some extent in contrast with Brunsell and Gilles (2003). Possibly the weak-wind situation, with mean wind speeds that did not exceed $5\,\mathrm{m\,s^{-1}}$ during the flights, allowed an effect of the surface heterogeneity up to unexpected large heights.

Also large horizontal variability of the latent heat flux λE was observed, but a systematic dependence on the surface type was not identified. To some extent this was due to the larger statistical error of λE, though generally the latent heat flux seemed

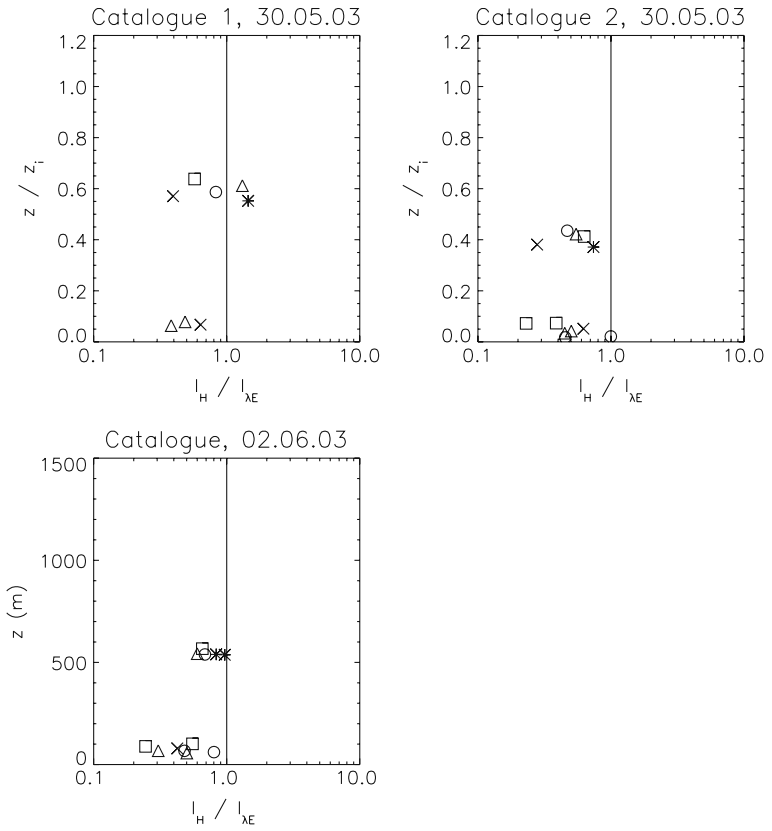

Fig. 13 Vertical profiles of integral scale ratio measured during LITFASS-2003. From top left to bottom: flight L11, L12, L13. For the explanation of the symbols, see Fig. 3

to be disconnected to the surface structures or to convective updrafts and downdrafts at 80 m agl anymore.

Cross-correlation coefficients $r_{w\theta}$ and r_{wm} did not depend on the underlying surface, except for the forest that gave $r_{w\theta} \approx 0.6$ on most flights. Sensible heat was in general transported more efficiently than moisture, in agreement with surface-layer observations (Katul and Hsieh 1999; Roth and Oke 1995). But unlike in the surface-layer, also the opposite ($r_{w\theta} < r_{wm}$) was observed in our data: when $r_{w\theta}$ dropped below 0.3 over wet soil, the correlation of the vertical wind with the mixing ratio was quite pronounced. The relative transport efficiency r over wet soil decreased linearly with height from 1.5 at surface level to zero at $0.8z_i$ where entrainment became relevant. Above the lake the smallest transport efficiencies were found. The perception that the correlation coefficient for temperature and moisture $r_{\theta m}$ decreases from 1 at surface level to -1 at the top of the CBL was only roughly affirmed, especially below $0.6z_i$. On flights during a pronounced dry period even anti-correlation above the cool lake surface was found. The comparison of the moisture–temperature correlation with the relative transport efficiency clearly showed that $r > r_{\theta m}$.

The integral length scales for latent heat ($I_{\lambda E}$) was larger than I_H on most flights above soil and mixed surface. This explains why the statistical flux error of λE was

generally larger than the measured uncertainty of the sensible heat flux, excluding the flights above the lake. No dependence of the integral scales on the underlying surface was found, except for the flights during the dry period, when $I_{\lambda E}$ was clearly larger than I_H near the surface. This explains why the statistical error of the airborne moisture flux measurements at the lowest flight level were maximal when the soil contained little water.

The analysis of the airborne measurements during LITFASS-2003 and STINHO-2 has demonstrated that a remarkable gap exists between theoretical considerations and observations when it comes to atmospheric flow above a heterogeneous surface. The vertical reach of the surface heterogeneity into the CBL was surprisingly large, and the interplay between sensible heat and water vapour ranged from fairly correlated to de-coupled. More experimental data on this topic and LES studies containing air moisture and realistic terrain (as already initiated by Uhlenbrock et al. 2004) would certainly help to enhance the understanding.

Acknowledgements The authors thank Peter Zittel for the data preparation and the work in the field. Our special thanks to Lothar Hartmann, Wolfgang and Franz Josef Strathausen (FJS Helicopter Service) for 100 perfect flight hours. We thank the coordinator of EVA_GRIPS, Theo Mengelkamp, and the coordinator of VERTIKO, Christian Bernhofer. This work was funded by the BMBF (German Federal Ministry for Education and Research), contract No. 07ATF37 (VERTIKO) and 01LD0301 (EVA_GRIPS). Important parts of the analysis were funded by the Technical University of Dresden, and performed at the Centre of Excellence in Small-Scale Atmospheric Research (CESSAR) in Warsaw, supported by the European Commission (EVK2-CT-2002-80010).

References

Bange J, Beyrich F, Engelbart DAM (2002) Airborne measurements of turbulent fluxes during LITFASS-98: a case study about method and significance. Theor Appl Climatol 73:35–51

Bange J, Roth R (1999) Helicopter-borne flux measurements in the nocturnal boundary layer over land—a case study. Boundary-Layer Meteorol 92:295–325

Bange J, Spieß T (2006) Airborne measurements in the early-morning shallow convective boundary layer. In: 17th symposium on boundary layers and turbulence. San Diego, CA, USA, 11 pp.

Bange J, Spieß T, Zittel P (2004) New method for the determination of turbulent surface fluxes from low-level flights: verification and benefit in joint field experiments. In: AMS: Eighth symposium on integrated observing and assimilation systems for atmosphere, oceans, and land surface. Seattle, USA, 1.6, 6 pp.

Bange J, Zittel P, Spieß T, Uhlenbrock J, Beyrich F (2006) A new method for the determination of area-averaged turbulent surface fluxes from low-level flights using inverse models. Boundary-Layer Meteorol DOI: 10.1007/s10546-005-9040-6

Beyrich F, Herzog H-J, Neisser J (2002) The LITFASS Project of DWD and the LITFASS-98 Experiment: the project strategy and the experimental setup. Theor Appl Climatol 73:3–18

Beyrich F, Leps J-P, Mauder M, Bange J, Foken T, Huneke S, Lohse H, Lüdi A, Meijninger WML, Mironov UWD, Zittel P (2006) Area-averaged surface fluxes over the LITFASS area from eddy-covariance measurements. Boundary-Layer Meteorol In press

Beyrich F, Mengelkamp H-T (2006) Evaporation over a heterogeneous Land Surface: EVA_GRIPS and the LITFASS-2003 Experiment—an Overview. Boundary-Layer Meteorol In press

Blackadar AK (1998) Turbulence and diffusion in the atmosphere. Springer, Berlin, Heidelberg, New York, 185 pp.

Bösenberg J, Linné H (2002) Laser remote sensing of the planetary boundary layer. Meteorol Z 11:233–240

Brunsell NA, Gilles RR (2003) Length scale analysis of surface energy fluxes derived from remote sensing. J Hydrometeorol 4:1212–1219

Claussen M (1991) Estimation of areally-averaged surface fluxes. Boundary-Layer Meteorol 54:387–410

Doran JC, Shaw WJ, Hubbe JM (1995) Boundary layer characteristics over areas of inhomogeneous surface fluxes. J Appl Meteorol 34:559–571

Engelbart DAM, Bange J (2002) Determination of boundary-layer parameters using wind profiler/RASS and Sodar/RASS in the frame of the LITFASS-Project. Theor Appl Climatol 73:53–65

Flamant C, Pelon J, Flamant PH, Durand P (1997) LIDAR determination of the entrainment zone thickness at the top of the unstable marine atmospheric boundary layer. Boundary-Layer Meteorol 83:247–284

Garratt JR (1990) The internal boundary layer—a review. Boundary-Layer Meteorol 50:171–203

Hennemuth B, Lammert A (2005) Determination of the atmospheric boundary layer height from radiosonde and lidar backscatter. Boundary-Layer Meteorol DOI: 10.1007/s10546-005-9035-3

Irvine MR, Gardiner BA, Hill MK (1997) The evolution of turbulence across a forest edge. Boundary-Layer Meteorol 84:467–496

Kaimal JC, Finnigan JJ (1994) Atmospheric boundary layer flows — Their structure and measurement, Oxford University Press, 289 pp.

Kalthoff N, Schädler G, Fiedler F, Adrian G (1993) Land surface processess over flat agricultural terrain: a comparison of measurements and simulation using LOTREX-10E/HIBE88 data. Meteorol Z N F 2:51–69

Katul GG, Hsieh C-I (1999) A note on the flux-variance similarity relationships for heat and water vapor in the unstable atmospheric surface layer. Boundary-Layer Meteorol 90:327–338

Klipp CL, Mahrt L (2003) Conditional analysis of an internal boundary layer. Boundary-Layer Meteorol 108:1–17

Kohsiek W, Meijninger WML, de Bruin HAR, Beyrich F (2005) Saturation of the large aperture scintillometer. Boundary-Layer Meteorol DOI: 10.1007/s10546-005-9031-7, 121

Lammert A, Bösenberg J (2006) Determination of the convective boundary layer height with laser remote sensing. Boundary-Layer Meteorol 119:159–170

LeMone MA, Grossman RL, Chen F, Ikeda K, Yates D (2003) Choosing the averaging interval for comparison of observed and modeled fluxes along aircraft transects over a heterogeneous surface. J Hydrometeorol 4:179–195

Lenschow DH, Mann J, Kristensen L (1994) How long is long enough when measuring fluxes and other turbulence statistics. J Atmos Oceanic Technol 11:661–673

Lenschow DH, Stankov BB (1986) Length scales in the convective boundary layer. J Atmos Sci 43:1198–1209

Linné H, Hennemuth B, Bösenberg J, Ertel K (2006) Water vapour flux profiles in the convective boundary layer. Theor Appl Climatol In Press

Lumley L, Panofsky H (1964) The structure of atmospheric turbulence. John Wiley & Sons, New York, 239 pp.

Mahrt L (1996) The bulk aerodynamic formulation over heterogeneous surfaces. Boundary-Layer Meteorol 78:87–119

Mahrt L (2000) Surface heterogeneity and vertical structure of the boundary layer. Boundary-Layer Meteorol 96:33–62

Mahrt L, Vickers D, Sun J (2001) Spatial variations of surface moisture flux from aircraft data. Adv Water Res 24:1133–1141

Mann J, Lenschow DH (1994) Errors in airborne flux measurements. J Geophys Res D 99:14519–14526

Maurer B, Heinemann G (2006) Validation of the lokal-Modell over heterogeneous land surfaces using aircraft-based measurements of the REEEFA experiment and comparison with micro-scale simulations. Meteorol Atmos Phys 91:107–128

Meijninger WML, Beyrich F, Lüdi A, Kohsiek W, de Bruin HAR (2005) Scintillometer-based turbulent fluxes of sensible and latent heat over a heterogeneous land surface—a contribution to Litfass-2003. Boundary-Layer Meteorol DOI: 10.1007/s10546-005-9022-8, 121

Morse AP, Gardiner BA, Marshall BJ (2002) Mechanisms controlling turbulence development across a forest edge. Boundary-Layer Meteorol 103:227–251

Muschinski A, Frehlich R, Jensen M, Hugo R, Hoff A, Eaton F, Balsley B (2001) Fine-scale measurements of turbulence in the lower troposphere: an intercomparison between a Kite- and Balloon-Borne, and a Helicopter-borne measurement system. Boundary-Layer Meteorol 98:219–250

Muschinski A, Wode C (1998) First in-situ evidence for co-existing sub-meter temperature and humidity sheets in the lower free troposphere. J Atmos Sci 55:2893–2906

Philip JR (1997) Blending and internal boundary-layer heights, and shear stress. Boundary-Layer Meteorol 84:85–98

Raabe A, Arnold K, Ziemann A, Beyrich F, Leps J-P, Bange J, Zittel P, Spieß T, Foken T, Göckede M, Schröter M, Raasch S (2005) STINHO—structure of turbulent transport under inhomogeneous surface conditions — part 1: the micro-α scale field experiment. Meteorol Z N F 14(3):315–327

Raupach MR, Finnigan JJ (1995) Scale issues in boundary-layer meteorology: surface energy balances in heterogeneous terrain. Hydrol Proc 9:589–612

Renfrew IA, King JC (2000) A simple model of the convective internal boundary layer and its application to surface heat flux estimates within polynyas. Boundary-Layer Meteorol 94:335–356

Roth M, Oke TR (1995) Relative efficiencies of turbulent transfer of heat, mass, and momentum over a patchy urban surface. J Atmos Sci 52:1863–1874

Roth R, Hofmann M, Wode C (1999) Geostrophic wind, gradient wind, thermal wind, and the vertical windprofile—an exemplary analysis within a planetary boundary layer over Arctic Sea-Ice. Boundary-Layer Meteorol 92:327–339

Rotta JC (1972) Turbulente Strömungen. Eine Einführung in die Theorie und ihre Anwendung. Teubner, Stuttgart, 267 pp.

Roy SB, Avissar R (2000) Scales of response of the convective boundary layer to land-surface heteroeneity. Geophys Res Lett 27(4):533–536

Savelyev SA, Taylor PA (2005) Internal boundary layers: I. height formulae for neutral and diabatic flows. Boundary-Layer Meteorol 115:1–25

Strunin MA, Hiyama T, Asanuma J, Ohata T (2004) Aircraft observations of the development of thermal internal boundary layers and scaling of the convective boundary layer over non-homogeneous land surfaces. Boundary-Layer Meteorol 111:491–522

Uhlenbrock J, Raasch S, Hennemuth B, Zittel P, Meijninger W (2004) Effects of land surface heterogeneities on the boundary layer structure and turbulence during LITFASS-2003: large-eddy simulations in comparison with turbulence measurements. In: 16th symposium on boundary layers and turbulence. Portland/Maine, USA, 9.3, 4 pp.

Wieringa J (1986) Roughness-dependent geographical interpolation of surface wind speed averages. Quart J Roy Meteorol Soc 112:867–889

Wolff M, Bange J (2000) Inverse method as an analysing tool for airborne measurements. Meteorol Z N F 9:361–376

Wyngaard JC, Pennell WT, Lenschow DH, LeMone MA (1978) The temperature–humidity covariance budget in the convectice boundary layer. J Atmos Sci 35:47–58